

Nucleon pair approximation of the nuclear collective motion

Y. M. Zhao,^{1,4} S. Yamaji,¹ N. Yoshinaga,² and A. Arima³

¹*Cyclotron Laboratory, Institute of Physical and Chemical Research (RIKEN), Hirosawa 2-1, Wako-shi, Saitama, 351-0198, Japan*

²*Department of Physics, Saitama University, Urawa, Saitama, 338-0825, Japan*

³*The House of Councilors, 2-1-1 Nagatacho, Chiyodaku, Tokyo, 100-8962, Japan*

⁴*Department of Physics, Southeast University, Nanjing 210018, People's Republic of China*

(Received 21 December 1999; published 22 June 2000)

The nucleon pair shell model calculation is performed in terms of the SD collective pairs which are obtained in a suitable way to obtain the maximum collectivity. The method is applied to even-even Sn, Te, Xe, Ba, and Ce isotopes near the $A=130$ region employing the (monopole and quadrupole) pairing plus quadrupole-quadrupole-type interaction with a very few parameters. The structure of energy levels for the quasi- γ band as well as the ground band is well reproduced in each nucleus. Other properties such as $E2$ transition rates and binding energies also agree with experimental data very well. The overall fit with the experimental data is superior to the previous calculations.

PACS number(s): 21.10.Re, 21.60.Ev, 23.20.Js, 27.60.+j

I. INTRODUCTION

A central problem in nuclear structure theory is how to describe the collective and low-lying excitations in terms of the spherical shell model. As is well known, the dimension of the configuration space of the shell model increases very fast with the valence nucleon number, and becomes prohibitively huge for medium-heavy nuclei. As a consequence, one needs to seek a judicious truncation scheme, i.e., to select the collective configurations from the whole shell model space. During the past 20 years, countless calculations within the framework of the interacting boson model (IBM) have been done, and the model has proved to be a valuably interpretive and predictive aid in understanding the nuclear structure and its evolution. Through the great success of the IBM [1], it was recognized that the collective angular momentum zero (S) and two (D) pairs play a dominant role in the collective motions. In the IBM, the SD pairs are approximated as sd bosons. Another similar model, the fermion dynamical symmetry model (FDSM) [2], constructs the collective SD subspace using the $SP(6)$ or $SO(8)$ symmetry-dictated SD pairs. Besides the above two truncations, there were other truncation schemes along the same line, such as the broken pair approximations (BPA) [3], the favored pair approximations (FPA) [4], etc.

Recently, Chen generalized the Wick theorem which now applies to fermion pairs [5]. Based on this technique, he proposed a nucleon-pair shell model (NPSM) [6]. In the NPSM, nucleon pairs with various angular momenta are used as the building blocks of the truncated shell model space. The NPSM has several advantages. First, it is flexible enough to include the BPA, the FPA, and the FDSM as its special cases, i.e., the nucleon pairs in the NPSM may be arbitrarily constructed if necessary. Second, the Hamiltonian in the NPSM can take the single particle (s.p.) term H_0 into consideration, which is usually treated as a constant in the FPA and the FDSM. It is meaningful to include the H_0 term in the Hamiltonian H because the H_0 comes from the dominant part, namely, mean-field part in H . Third, since calculations are carried out within the nucleon pair subspace, one can

properly take into account the Pauli effect, which can be treated only by adjusting interaction strengths in the boson models. Fourth, through earlier investigations [13] it is proper to use S and D pairs in vibrational and transitional regions whereas we may need G pairs in deformed areas.

In this paper, we apply the NPSM to the Sn, Te, Xe, Ba, and Ce isotopes using the S and D pairs as its basic building blocks. In Sec. II we describe how to construct the multi-pair basis states using the collective S and D pairs. We assume a monopole and quadrupole pairing, and quadrupole-quadrupole interaction between like valence nucleons, and quadrupole-quadrupole interactions between valence protons and neutrons. In Sec. III the S pair is determined by solving the Bardeen-Cooper-Schrieffer (BCS) equation, and the D pair is related to the S pair via a commutation with quadrupole operator. Calculational results are given and compared with experimental data in Sec. IV. In Sec. V a discussion and conclusions are given. In Appendix A we discuss some of our innovative methods to improve our numerical calculations. In Appendix B we note the strengths of multipole pairing interaction and quadrupole-quadrupole force.

II. MULTIPAIR BASIS AND HAMILTONIAN

The collective pair of angular momentum r with its projection μ is defined as

$$A_{\mu}^{r\dagger} = \sum_{ab} y(abr) (C_a^{\dagger} \times C_b^{\dagger})_{\mu}^r, \quad (1)$$

$$y(abr) = -(-)^{a+b+r} y(bar),$$

where $r=0,2$ corresponds to the S and D pairs, respectively. C_a^{\dagger} and C_b^{\dagger} are single-particle creation operators. a and b denote all quantum numbers (except the magnetic quantum number) necessary to specify a state [$a \equiv (nlj)$]. We also use them to denote the angular momentum of the single particle orbit in case there is no confusion (i.e., a is used to label the single particle orbit as well as denote the corresponding j value.). $y(abr)$ are structure coefficients of the collective

pair, which should be determined via an appropriate procedure to maximize the collectivity of the S and D pairs. These nucleon pairs are coupled step by step to yield an N -pair basis

$$\begin{aligned} |\tau J_N M_N\rangle &\equiv A_{M_N}^{J_N} (r_i, J_i) |0\rangle, \\ A_{M_N}^{J_N} (r_1 r_2 \dots r_N, J_1 J_2 \dots J_N) &= [\dots (A^{r_1} \times A^{r_2})^{J_2} \times \dots \\ &\quad \times A^{r_N}]_{M_N}^{J_N}, \end{aligned} \quad (2)$$

where $J_1 = r_1$, J_N is the total angular momentum of the above N -pair operator, and M_N is the z projection of J_N . Here τ is an abbreviation for all the necessary intermediate quantum numbers. Details of choosing a complete set of the multipair basis states were discussed in Refs. [6,7]. It should be noted that for a fixed total number of S and D pairs the number of linear independent basis states for a given angular momentum J_N is definite, and is actually equal to that of the sd boson states, but there are various ways to choose intermediate angular momenta J_i ($i=2, \dots, N-1$) to make those basis states. For a given J_N , it would be better to choose the possible *smallest* value for each J_i for the sake of saving computing time (while in Ref. [7] possible largest values for J_i were taken). There are other techniques to save the computing time, which are presented in Appendix A.

The time inversed of the above N -pair operator is

$$\begin{aligned} \tilde{A}_{M_N}^{J_N} (r_1 r_2 r_3 \dots r_N, J_1 J_2 J_3 \dots J_N) &= \{\dots [(\tilde{A}^{r_1} \times \tilde{A}^{r_2})^{J_2} \times \tilde{A}^{r_3}]^{J_3} \\ &\quad \times \dots \times \tilde{A}^{r_N}\}_{M_N}^{J_N} \\ &\equiv \tilde{A}_{M_N}^{J_N} (r_i, J_i). \end{aligned} \quad (3)$$

\tilde{A}^{r_i} is defined as

$$\tilde{A}^{r_i} = (-) \sum_{ab} y(abr_i) (\tilde{C}_a \times \tilde{C}_b)^{r_i}, \quad (4)$$

where $\tilde{C}_{am} = \tilde{C}_{(nlj)m} = (-)^{j-m} C_{a-m}$, and C_{am} is the annihilation operator.

In this paper, the Hamiltonian is chosen as

$$H = H_0 + H_P + \kappa Q_\pi \cdot Q_\nu. \quad (5)$$

The first part is the spherical single-particle energy term

$$H_0 = \sum_{\alpha\sigma} \epsilon_{\alpha\sigma} C_{\alpha\sigma}^\dagger C_{\alpha\sigma}, \quad (6)$$

where α denotes all quantum numbers necessary to specify a state, $\alpha \equiv (nljm)$, and $\sigma = \pi, \nu$ corresponds to degree of freedom for protons and neutrons, respectively. The remaining two terms are residual interactions, and they are assumed to consist of the pairing plus quadrupole-quadrupole ($P+Q$) interaction [8]. H_P denotes monopole and quadrupole pairing, and quadrupole-quadrupole interaction between like valence nucleons, which is denoted as

$$H_P = V_0 + V_2 + V_Q, \quad (7)$$

where V_0 is the monopole pairing interaction:

$$V_0 = \frac{1}{4} \sum_{\sigma=\pi,\nu} \sum_{\alpha\gamma} G_{\sigma} s_{\alpha\sigma} s_{\gamma\sigma} C_{\alpha\sigma}^\dagger C_{\bar{\alpha}\sigma}^\dagger C_{\bar{\alpha}\sigma} C_{\gamma\sigma}. \quad (8)$$

s_α here is a sign $s_{\alpha\sigma} = (-)^{j_\sigma - m_\sigma}$, which is related to the time-reversal properties of the states, $\bar{\alpha} = (nlj - m)$. V_0 can be rewritten as

$$V_0 = G_\pi \mathcal{P}_\pi^\dagger \mathcal{P}_\pi + G_\nu \mathcal{P}_\nu^\dagger \mathcal{P}_\nu, \quad (9)$$

where

$$\mathcal{P}_\sigma^\dagger = \sum_{a_\sigma} \frac{\hat{j}_\sigma}{2} (C_{a_\sigma}^\dagger \times C_{a_\sigma}^\dagger)_0, \quad (10)$$

with $\hat{j} = (2j+1)^{1/2}$. V_2 in Eq. (7) is a quadrupole pairing force,

$$V_2 = \sum_{\sigma} G_{\sigma}^2 \mathcal{P}_{\sigma}^{(2)\dagger} \cdot \mathcal{P}_{\sigma}^{(2)}, \quad (11)$$

where $\mathcal{P}_{\sigma}^{(2)\dagger}$ is defined as

$$\mathcal{P}_{\sigma M}^{(2)\dagger} = \sum_{a_\sigma b_\sigma} q(a_\sigma b_\sigma) (C_{a_\sigma}^\dagger \times C_{b_\sigma}^\dagger)_M^2, \quad (12)$$

with $M = 0, \pm 1, \pm 2$; $q(a_\sigma b_\sigma)$ is the same as what appears in the Q_σ operator in Eq. (14), which is defined as

$$Q_M = \sum_{\alpha\gamma} \langle \alpha | r^2 Y_M^2 | \gamma \rangle C_{\alpha}^\dagger C_{\gamma}, \quad (13)$$

where $\gamma \equiv (nl'j'm') = (bm')$. Note that the script $\sigma = \pi$ or ν is omitted in the above definition since Q is just $r^2 Y_M^2$, and it has the same form for protons and neutrons. Via some recoupling techniques of angular momentum, it is easy to rewrite Q as

$$Q_M = \sum_{ab} q(ab) (C_a^\dagger \times \tilde{C}_b)_M^2, \quad (14)$$

with

$$q(ab) = \frac{(-)^{j+1/2}}{\sqrt{20\pi}} \hat{j} \hat{j}' C_{j_1/2, j_2, j_3, -1/2}^{20} \langle nl | r^2 | nl' \rangle,$$

where $C_{j_1/2, j_2, j_3, -1/2}^{20}$ is the Clebsch-Gordan coefficient. The matrix elements of r^2 are given in [9]:

$$\begin{aligned} \langle nl | r^2 | nl' \rangle &= \begin{cases} (n+3/2)r_0^2, & l=l' \\ (n+l'+2\pm 1)^{1/2} (n-l'+1\mp 1)^{1/2} r_0^2, & l=l'\pm 2, \end{cases} \end{aligned} \quad (15)$$

where $r_0^2 = \hbar/M_N\omega_0 = 1.012 \text{ \AA}^{1/3} \text{ fm}^2$. M_N is the mass of a nucleon, and ω_0 is the harmonic-oscillator frequency. We do not use the actual value of r_0^2 when we calculate the excitation energies and binding energies in this paper, but quadrupole pairing and quadrupole interaction strengths are given in unit of MeV/r_0^4 . The matrix elements of r^2 are used in calculating $E2$ transitions.

V_Q in Eq. (7) is a quadrupole-quadrupole interaction between like valence nucleons,

$$V_Q = \sum_{\sigma} \kappa_{\sigma} Q_{\sigma} \cdot Q_{\sigma}. \quad (16)$$

The $E2$ transition operator is

$$T(E2) = e_{\pi} Q_{\pi} + e_{\nu} Q_{\nu}, \quad (17)$$

where e_{ν} and e_{π} are effective charges of valence neutrons and protons which include their bare charges, respectively.

The numerical code of the SD pair shell model for even-even nuclei was written in *C* language [10,11]. The input includes the single-particle energies, the parameters of the Hamiltonian, and effective charges. The output includes the energies for the ground state, low-lying excitation states, and the $E2$ ($M1$) transition rates among these states, radii of nuclei, and so on.

III. PARAMETERS IN THE HAMILTONIAN

Now we come to the question of the structure coefficients of the collective S and D pairs. For given pairing strengths G_{ν} and G_{π} we solve the BCS equation to obtain u_a and v_a , the empty and occupied amplitudes, respectively, for orbit a . Then the collective S pair is defined to be [12]

$$S^{\dagger} = \sum_a y(aa0) (C_a^{\dagger} \times C_a^{\dagger})^0, \quad y(aa0) = \hat{a} \frac{v_a}{u_a}. \quad (18)$$

The D pair is obtained by using the commutator [12]

$$D^{\dagger} = \frac{1}{2} [Q, S^{\dagger}] = \sum_{ab} y(ab2) (C_a^{\dagger} \times C_b^{\dagger})^2. \quad (19)$$

Here operator Q is defined in Eq. (14). From Eq. (19), it is easy to obtain (after symmetrization)

$$y(ab2) = -\frac{1}{2} q(ab) \left[\frac{y(aa0)}{\hat{a}} + \frac{y(bb0)}{\hat{b}} \right]. \quad (20)$$

There are also other ways to define D pair [13], but it is expected that Eq. (19) is one of the best ways when the quadrupole-quadrupole interaction between protons and neutrons are strong. In some magic or near magic nuclei where interactions between like particles are important compared with those between unlike particles, we must seek for other methods. Note that we omitted the script σ in Eqs. (18)–(20) since we determine the SD pairs separately for protons and neutrons in the same way, and this omission does not cause confusion.

Prior to this work, there were some calculations of the nuclei in the same region, e.g., microscopic calculations [14] by the IBM using OAI mapping [15], and several tentative calculations in the SD pair shell model using similar SD nucleon pairs [7,16,17]. The main difference of this work with [14] is that only two D pairs were involved in the SD pair subspace in Ref. [14], since the boson mapping requires only up to two D pairs, and here we have D pairs as many as possible, that is, we have taken into account the entire SD subspace. The difference from Refs. [7,17] is that of the SD truncation procedure and the form of the Hamiltonian. The difference from Ref. [16] is the form of the Hamiltonian, and the procedures in adjusting parameters, which leads to substantial improvements of the agreement with experimental data, and will be explained below.

In Ref. [7], Chen and co-workers used several methods to truncate the shell model space to the SD subspace, then carried out calculations on the nucleus ^{134}Ba in the SD subspace. They used two kinds of interactions between like valence nucleons, the monopole pairing or the surface delta interaction (SDI) V_{SDI} . In Ref. [17] the authors used V_{SDI} between like valence nucleons, and the collective S and D pairs were constructed by diagonalizing the SDI Hamiltonian ($H_{\text{SDI}} = \sum_{\alpha} \epsilon_{\alpha} C_{\alpha}^{\dagger} C_{\alpha} + V_{\text{SDI}}$) in the basis $(C_a^{\dagger} \times C_b^{\dagger})r|0\rangle$, that is, in the two-particle space. As a consequence, the many-body effect on the structure of the S and D pairs was ignored, i.e., the structure coefficients $y(abr)$'s of the collective S and D pairs do not change with the pair numbers. Another point is that in Ref. [17] the parameters changed rapidly as a function of neutron pairs. In Refs. [7,17] the parameters for the interactions were quite different for protons and neutrons, the strength of the quadrupole-quadrupole interaction between protons and neutrons is too strong (e.g., $\kappa = -0.212 \text{ MeV}/r_0^4$ for the nucleus ^{134}Ba). In Ref. [7] a smaller value of κ was taken for the so-called ‘‘SDI-B,’’ ‘‘HFB,’’ and ‘‘BCS’’ truncations, but the $E2$ transitions for these truncations completely contradicted with the experimental data. In Refs. [11,16] parameters of the pairing strengths G_{π} and G_{ν} in the monopole pairing [Eq. (9)] were rather weak in order to obtain reasonable agreement with the experimental data. The reason for this is that the contribution from the quadrupole pairing and the quadrupole-quadrupole interactions between like nucleons, which are not negligible, was omitted therein. Even if the pairing parameters of the Hamiltonian were ‘‘modified’’ in this way, the fit of energy levels and the electromagnetic transition rates among them with experimental data was not good [11,16]. In fact, if one uses the Hamiltonian, excluding the quadrupole pairing and the quadrupole-quadrupole force between like nucleons, and meanwhile uses the guide values for the parameters of the BCS equation, for example, -0.18 MeV for G_{π} and -0.13 MeV for G_{ν} , as done in Ref. [6], one would obtain very large excitation energies for the low-lying states [e.g., $E_{2_1^+} = 1.845$, $E_{4_1^+} = 3.800$, and $E_{6_1^+} = 5.933$ (in MeV) for the nucleus ^{134}Ba if $\kappa = 0.08 \text{ MeV}/r_0^4$]. In order to have a reasonable excitation, one has to use much smaller monopole pairing strengths, as done in Refs. [11,16]. For these reasons, the above SD truncation of the shell model was almost con-

TABLE I. Single-particle energies for protons (particlelike) and neutrons (holelike) adopted from Refs. [18,19].

| j | $s_{1/2}$ | $d_{3/2}$ | $d_{5/2}$ | $g_{7/2}$ | $h_{11/2}$ |
|----------------------|-----------|-----------|-----------|-----------|------------|
| ϵ_π (MeV) | 2.990 | 2.690 | 0.963 | 0 | 2.76 |
| ϵ_ν (MeV) | 0.332 | 0.000 | 1.655 | 2.434 | 0.242 |

cluded [7] not to be a good candidate of the SD truncation scheme, although it was suggested to be in previous studies [12]. In addition, the BCS equation is unstable for small (≤ 0.01) and large N ($N \geq 4$) pairing strengths, which makes the SD truncation method in this paper completely inapplicable for large N if one uses the BCS pair as the S pair and uses a Hamiltonian without quadrupole pairing interaction and quadrupole-quadrupole interaction between like valence nucleons at the same time. Another disadvantage of the calculations neglecting the quadrupole pairing and quadrupole-quadrupole interaction between like valence nucleons [16] is that it is difficult to obtain ‘‘reasonable’’ systematics within the ‘‘valence correlation scheme’’ defined by Casten and Zamfir [18]. The calculated $E_{2_1^+}$ would drop with $N_\pi N_\nu$ at a ‘‘speed’’ [16] which is much slower than the behavior of the experimental data. Effective charges were rather large ($e_\pi = e_\nu = 2.1\epsilon$ in Refs. [7,17], for example) to obtain a reasonable agreement with one or two nuclei, but the calculated $E2$ transitions rates increased very slowly with the neutron pair number, which contradicted the experimental data. Another important difference between this work and the previous calculations within the SD nucleon pair shell model [7,11,16,17] is that we use positive neutron-proton quadrupole-quadrupole strength κ in this paper because we treat neutron-deficient nuclei. This is different from the previous calculations [7,11,16,17], where a negative κ was used. The reason is that the operator Q_ν changes its sign due to the particle-hole transformation, or equivalently, one should use positive κ in the parameterization of the shell model calculations. Another interesting point is on the proton-neutron quadrupole-quadrupole interaction strength, κ . We note that the best-fit κ changes very little for nuclei involved here. In order to reduce the number of parameters, we use a fixed value ($\kappa = 0.06 \text{ MeV}/r_0^4$) throughout this paper.

The neutron single-particle energies are taken from experimental data [19], and the proton single-particle energies are obtained from an extension of available experimental data [20], as shown in Table I. The parameters of the Hamiltonian in this paper are listed in Table II. It is interesting to note that the parameters for quadrupole pairing and the quadrupole-quadrupole force are comparable with the effective interaction in Ref. [21] if the difference in definitions for quadrupole pairing and the quadrupole operator is taken into consideration. In this paper, we set $G_\pi^2 = G_\nu^2$ and $\kappa_\pi = \kappa_\nu$ for the sake of simplicity. These are the only two independent parameters which are varied in a reasonable range for nuclei under consideration in this paper. Other parameters such as the monopole pairing strengths are fixed for all nuclei. For the sake of conveniences, different definitions on pairing in-

TABLE II. Parameters ($G_\sigma^2, \kappa_\sigma$) in (MeV/r_0^4) used in the Hamiltonian. We set $G_\pi = -0.180 \text{ MeV}$, $G_\nu = -0.131 \text{ MeV}$, and $\kappa = 0.06 \text{ MeV}/r_0^4$ for all the nuclei. The parameters in this work are comparable to those of the $P+Q$ model, where $G_\sigma m f \sim -0.150 \text{ MeV}$, $G_\sigma^2 \sim 0.03 \text{ MeV}/r_0^4$, and $|\kappa| \sim \frac{1}{2} |\kappa_\sigma| \sim 0.07 \text{ MeV}/r_0^4$.

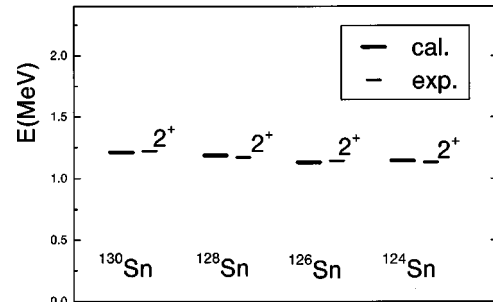
| Nucl. | ^{132}Sn | ^{130}Sn | ^{128}Sn | ^{126}Sn | ^{124}Sn |
|-----------------|-------------------|-------------------|-------------------|-------------------|-------------------|
| G_σ^2 | - | -0.013 | -0.014 | -0.016 | -0.015 |
| κ_σ | - | -0.015 | -0.015 | -0.015 | -0.020 |
| Nucl. | ^{134}Te | ^{132}Te | ^{130}Te | ^{128}Te | ^{126}Te |
| G_σ^2 | -0.024 | -0.020 | -0.020 | -0.023 | -0.025 |
| κ_σ | -0.025 | -0.017 | -0.021 | -0.024 | -0.025 |
| Nucl. | ^{136}Xe | ^{134}Xe | ^{132}Xe | ^{130}Xe | ^{128}Xe |
| G_σ^2 | -0.024 | -0.022 | -0.025 | -0.028 | -0.029 |
| κ_σ | -0.025 | -0.025 | -0.026 | -0.028 | -0.029 |
| Nucl. | ^{138}Ba | ^{136}Ba | ^{134}Ba | ^{132}Ba | ^{130}Ba |
| G_σ^2 | -0.018 | -0.021 | -0.025 | -0.030 | -0.032 |
| κ_σ | -0.045 | -0.045 | -0.045 | -0.045 | -0.045 |
| Nucl. | ^{140}Ce | ^{138}Ce | ^{136}Ce | ^{134}Ce | ^{132}Ce |
| G_σ^2 | -0.019 | -0.021 | -0.025 | -0.030 | -0.032 |
| κ_σ | -0.045 | -0.045 | -0.045 | -0.040 | -0.045 |

teraction and quadrupole-quadrupole interaction are explained and compared in Appendix B.

IV. CALCULATIONAL RESULTS

A. Energy spectra and $B(E2)$

Hamiltonian (5) is believed to include all the essential ingredients of physics, and it is expected to describe the general features of the low-lying excitations well if the SD truncation is good. A comparison between the calculated 2_1^+ state and the experimental data for the Sn isotopes is given in Fig. 1, and the calculational spectra of other isotopes are compared with the experimental data in Fig. 2. It is easy to notice that the low-lying energy levels on the ground band and the quasi- γ band are reasonably reproduced. The quasi- β bandhead energies are also nicely reproduced. In most studies of the previous SD nucleon pair shell model calculations [7,11,16,17], the level sequences in the quasi- γ band were

FIG. 1. The 2_1^+ states of Sn isotopes.

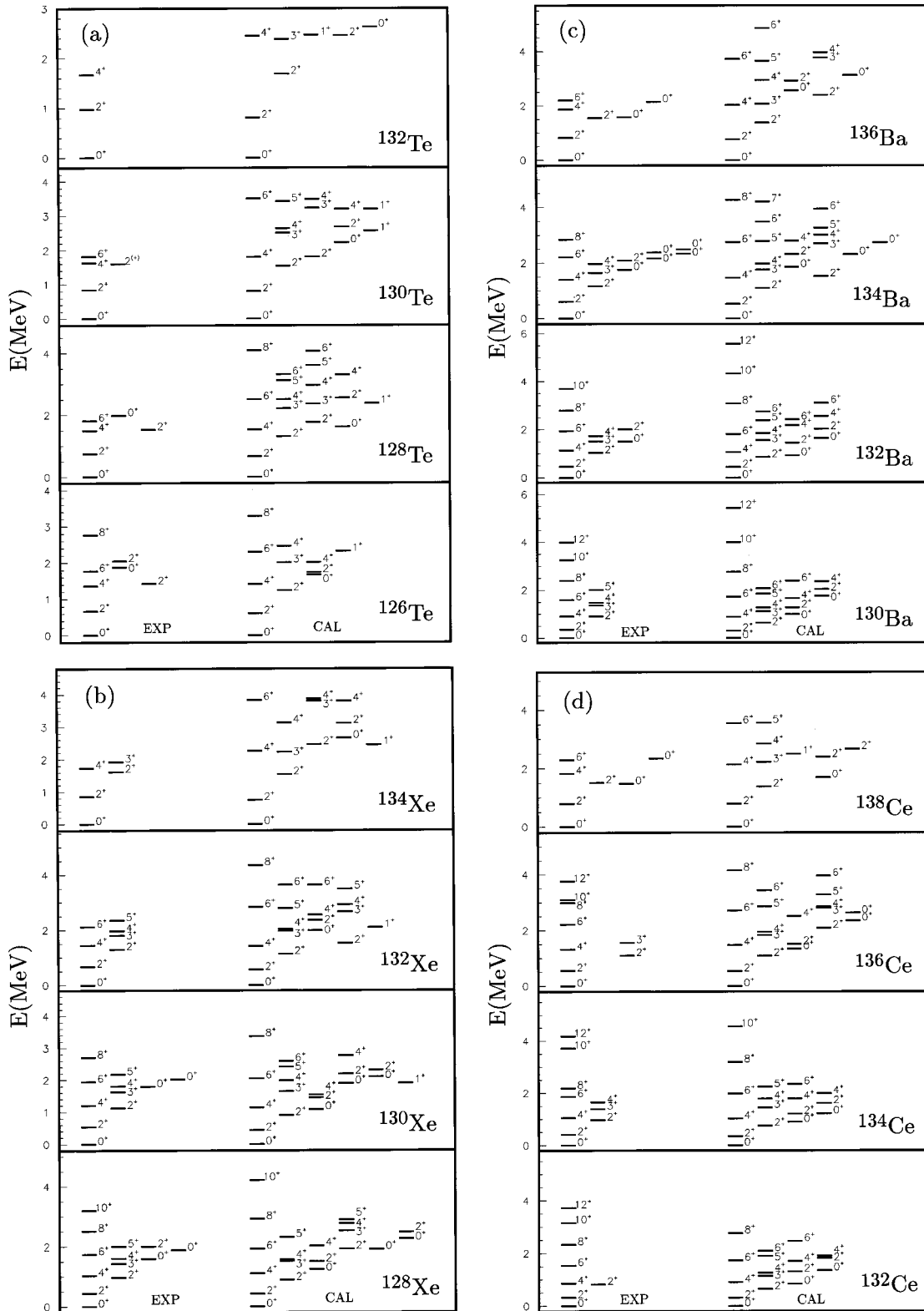


FIG. 2. The spectra of Te (a), Xe (b), Ba (c), and Ce (d) isotopes. Left-hand side, experimental data (taken from Ref. [22]); right-hand side, calculated spectra.

not correctly reproduced. The only exception is that the BCS truncation in Ref. [7] predicted the correct position of the 3_1^+ state, but the $E2$ properties therein were completely different from the experimental data. In the case of $N_\pi N_\nu \leq 3$, the SD

subspace was not believed to be a good approximation of the shell model space [7], where the contribution from the other configurations such as the collective G pair may not be negligible. The 6^+ state on the ground band for the nuclei

TABLE III. The relative $B(E2)$ values for $^{130,132,134}\text{Ba}$ and $^{128,130}\text{Xe}$. The experimental data are taken from Ref. [16]. O(6) means the relative $B(E2)$ transitions of the IBM prediction in the O(6) limit. In this table we use effective charges $e_\pi = -e_\nu = 1.6e$.

| Nucl. $J_i \rightarrow J_f$ | ^{132}Ba | | ^{134}Ba | | ^{130}Xe | | ^{130}Ba | | ^{128}Xe | | |
|--------------------------------|-------------------|-------|-------------------|-------|-------------------|-------|-------------------|-----------|-------------------|-------|-------|
| | O(6) | Expt. | Cal. | Expt. | Cal. | Expt. | Cal. | Expt. | Cal. | Expt. | Cal. |
| $2_2^+ \rightarrow 2_1^+$ | 100 | 100 | 100 | 100 | 100 | 100 | 100 | 100 | 100 | 100 | 100 |
| $\rightarrow 0_1^+$ | 0 | 0.2 | <0.1 | 0.6 | 0.5 | 8 | <0.1 | 5.7 | <0.1 | 1.2 | 0.2 |
| $3_1^+ \rightarrow 2_2^+$ | 100 | 100 | 100 | 100 | 100 | 100 | 100 | 100 | 100 | 100 | 100 |
| $\rightarrow 4_1^+$ | 40 | 73 | 34.4 | 40 | 31.5 | 25 | 36.1 | 30 | 35.9 | 37 | 35.4 |
| $\rightarrow 2_1^+$ | 0 | 0.2 | <0.1 | 1.0 | 1.3 | 1.4 | 1.2 | 1.5 | <0.1 | 1 | 1.1 |
| $4_2^+ \rightarrow 2_2^+$ | 100 | 100 | 100 | 100 | 100 | 100 | 100 | 100 | 100 | 100 | 100 |
| $\rightarrow 3_1^+$ | 0 | - | <0.1 | 14.5 | 9.2 | - | <0.1 | - | 4.5 | - | 9.6 |
| $\rightarrow 4_1^+$ | 91 | 75 | 97.1 | 77 | 84.1 | 107 | 111.0 | 89 | 101.6 | 133 | 108.4 |
| $\rightarrow 2_1^+$ | 0 | 2.2 | 1.4 | 2.5 | 5.6 | 3.2 | 4.9 | 3.9 | 1.7 | 1.7 | 5.6 |
| $5_1^+ \rightarrow 3_1^+$ | 100 | 100 | 100 | 100 | 100 | 100 | 100 | 100 | 100 | 100 | 100 |
| $\rightarrow 4_2^+$ | 46 | - | 53.9 | - | 67.8 | - | 35.1 | ≤ 57 | 64.4 | 88 | 45.0 |
| $\rightarrow 6_1^+$ | 45 | - | 41.2 | - | 49.0 | - | 28.7 | 381 | 43.9 | 204 | 29.2 |
| $\rightarrow 4_1^+$ | 0 | - | 0.6 | - | 3.0 | - | 9.5 | 6.7 | 1.0 | 3.7 | 7.2 |
| $0_2^+ \rightarrow 2_2^+$ | 100 | 100 | 100 | 100 | 100 | 100 | 100 | 100 | 100 | 100 | 100 |
| $\rightarrow 2_1^+$ | 0 | 0 | 1.0 | 4 | 11.1 | 2.6 | 2.6 | - | 0.3 | 14 | 0.2 |

$^{130,128}\text{Te}$, ^{132}Te , ^{136}Ba , and ^{138}Ce is not reproduced in this paper because it is a precollective state, namely, a state where seniority scheme works rather well and nuclear collectivity is not dominant. The $J \geq 8$ states of the nuclei $^{134,136}\text{Ce}$ are not satisfactorily reproduced, where the calculated levels are higher than the experimental data. Those states are not highly collective excitations.

In order to fit the experimental data of the $E2$ transition rates, one may adjust the effective charges. In this paper we fix the $e_\pi = 1.6e$ and $e_\nu = -1.6e$ for all nuclei. Note that e_ν is in opposite sign to proton effective charge because we choose the holelike picture for the neutron SD subspace. The calculated relative $B(E2)$'s are compared with the experimental data [23] and the predictions of the IBM O(6) limit in Table III. The behavior of relative $B(E2)$ is interesting since it can be used to examine the main features of the wave function for these nuclei. It is easy to notice that main features for the nuclei $^{134,132}\text{Ba}$ and ^{130}Xe , which were pointed out to display the O(6) symmetry of the IBM [23], are nicely reproduced by adjusting only κ_σ and G_σ^2 . Compared with previous results [7,11,16,17], the fit between the calculational results and experimental data is substantially improved. Particularly, the $E2$ transition rates of $B(E2, 0_1^+ \rightarrow 2_1^+)$ for most nuclei are reasonably reproduced using constant and reasonable parameters of the effective charge, while the previous calculations within the SD -pair subspace [7,11,16,17] could not. We would like to mention that we have tested different sets of effective charges (e.g., $e_\pi/e_\nu \sim 1.5$), and found the calculated relative $E2$ transition rates have very weak dependence on the specific choice of the ratio e_π/e_ν . In order to see how good the nucleon pair approximation can be in the nuclear collective motion we adjusted the proton and neutron effective charges using the least-square-fitting method. The best proton effective charge

is $e_\pi = 1.73035e$. and the best neutron effective charge is $e_\nu = -1.41201e$. The calculated results are shown in Table IV, labeled by Cal. 2. Like all the studies of the $B(E2)$ values using local, regional, and global systematics edited in Ref. [24], the abnormal ‘‘jump’’ of $B(E2, 0_1^+ \rightarrow 2_1^+)$ from the nucleus ^{134}Ce to the nucleus ^{132}Ce is not reproduced, and we excluded the experimental data in our least-square-fitting procedure. Here we say there is an abnormal $B(E2)$ ‘‘jump’’ in the experimental data of the nucleus ^{132}Ce because the experimental $B(E2)$ value of the nucleus ^{132}Ce ($1.77e^2b^2$) is much larger than that of the nucleus ^{134}Ce and is even larger than that of the nucleus ^{130}Ce ($1.73e^2b^2$). It is also interesting to note that parameter κ_σ affects the calculational spectra slightly but it cannot be neglected in order to reproduce the relative $E2$ transition rates. We point out that the experimental data for the $E2$ transition are still scarce. The $B(E2)$ data of $5_1^+ \rightarrow 3_1^+$, 6_1^+ , 4_1^+ , and 4_2^+ will be very useful not only for further identification of the O(6) property for the nuclei $^{134,132}\text{Ba}$ and ^{132}Xe , but also for checking the exactness of the SD truncation of the nuclear shell model in this paper.

B. Other properties

We have also calculated several other properties. Here we discuss two properties, nuclear radii and binding energies. In this paper, the r_σ^2 is defined as

$$\begin{aligned}
 \overline{r_\sigma^2} = & \frac{1}{Z_\sigma} \left[\sum_{i=1}^{Z_\sigma^0} \langle \Phi_0 | r_i^2 | \Phi_0 \rangle \right. \\
 & \left. + \delta_\sigma \langle 0_1^+ | \left(\sum_{\alpha_\sigma} \langle \alpha_\sigma | r^2 | \alpha_\sigma \rangle C_{\alpha_\sigma}^\dagger C_{\alpha_\sigma} \right) | 0_1^+ \rangle \right], \quad (21)
 \end{aligned}$$

TABLE IV. The calculated $B(E2, 0_1^+ \rightarrow 2_1^+)$ (in unit of $e^2 b^2$) using the S and D pair approximations in this paper. We used $e_\pi = -e_\nu = 1.6e$ in Cal.1. To see how good the S and D pair approximations could be, we adjusted the effective charges using a least-square-fitting procedure and recalculated the $E2$ transition rates, which are shown in Cal.2. The new effective charges are $e_\pi = 1.73035e$ and $e_\nu = -1.41201e$ in Cal.2. The mean standard error χ of the quantity $100 [B(E2, 0_1^+ \rightarrow 2_1^+)/A^{2/3}]^{1/2}$ in Cal.1 and Cal.2 is $1322e$ b and $1.018e$ b, respectively. The experimental data are taken from Ref. [24].

| | | | | | |
|-------|-------------------|-------------------|-------------------|-------------------|-------------------|
| Nucl. | ^{134}Te | ^{132}Te | ^{130}Te | ^{128}Te | ^{126}Te |
| Cal.1 | 0.117 | 0.251 | 0.432 | 0.565 | 0.652 |
| Cal.2 | 0.138 | 0.217 | 0.371 | 0.483 | 0.554 |
| Expt. | - | - | 0.295 ± 0.007 | 0.383 ± 0.006 | 0.475 ± 0.010 |
| Nucl. | ^{136}Xe | ^{134}Xe | ^{132}Xe | ^{130}Xe | ^{128}Xe |
| Cal.1 | 0.177 | 0.320 | 0.551 | 0.735 | 0.854 |
| Cal.2 | 0.205 | 0.289 | 0.498 | 0.655 | 0.756 |
| Expt. | 0.18 ± 0.08 | 0.34 ± 0.06 | 0.46 ± 0.03 | 0.65 ± 0.05 | 0.75 ± 0.04 |
| Nucl. | ^{138}Ba | ^{136}Ba | ^{134}Ba | ^{132}Ba | ^{130}Ba |
| Cal.1 | 0.231 | 0.414 | 0.717 | 0.946 | 1.117 |
| Cal.2 | 0.278 | 0.398 | 0.667 | 0.872 | 1.065 |
| Expt. | 0.226 ± 0.009 | 0.400 ± 0.005 | 0.680 ± 0.016 | 0.86 ± 0.06 | 1.29 ± 0.14 |
| Nucl. | ^{140}Ce | ^{138}Ce | ^{136}Ce | ^{134}Ce | ^{132}Ce |
| Cal.1 | 0.258 | 0.465 | 0.805 | 1.007 | 1.256 |
| Cal.2 | 0.308 | 0.443 | 0.760 | 0.935 | 1.252 |
| Expt. | 0.296 ± 0.006 | - | - | 1.03 ± 0.09 | 1.77 ± 0.14 |

where Z_σ ($\sigma = \pi$ or ν) is the proton number or neutron number of the nucleus, and Z_σ^0 is the nearest magic number for protons and neutrons; $|\Phi_0\rangle$ is the wave function of the core and $|0_1^+\rangle$ is the wave function of the ground state within the valence SD subspace; and $\delta_\sigma = +1(-1)$ if the corresponding valence space is constructed by the particle-like (hole-like) configurations. It is expected that the core be occupied completely, and the contribution from the core can be evaluated one by one using Eq. (15). The contribution from the valence nucleons (holes) can be calculated by rewriting $\sum_{\alpha_\sigma} \langle \alpha_\sigma | r^2 | \alpha_\sigma \rangle C_{\alpha_\sigma}^\dagger C_{\alpha_\sigma}$ in second-quantized form:

$$\sum_{\alpha_\sigma} \langle \alpha_\sigma | r^2 | \alpha_\sigma \rangle C_{\alpha_\sigma}^\dagger C_{\alpha_\sigma} = - \sum_{\alpha_\sigma} \hat{j} \left(n + \frac{3}{2} \right) r_0^2 (C_{\alpha_\sigma}^\dagger \times \tilde{C}_{\alpha_\sigma})^0. \quad (22)$$

$r_\sigma = \sqrt{r_\sigma^2}$ are presented and compared with the RMF results [26] in Table V. They are very consistent with each other.

The binding energies B are defined as

$$B = B_0 + \langle H_0 \rangle + \langle H_P \rangle + \langle \kappa Q_\pi \cdot Q_\nu \rangle, \quad (23)$$

where the constant parameter B_0 is determined so that the binding energy of the nucleus ^{132}Sn is equal to 0. We present the relative binding energies of these nuclei in Fig. 3. Note that we use two additional parameters to fix the place of single-particle levels (or, in other words, Fermi energies for proton and neutron). In this paper we set $\epsilon_{7/2_\pi} = -7.6$ MeV and $\epsilon_{7/2_\nu} = -7.8$ MeV. From Fig. 3 it is easy to notice that

the agreement between the calculated binding energies and the corresponding experimental data are reasonably good except for the nucleus ^{132}Ce . One possible explanation for the difference in binding energy of the nucleus ^{132}Ce is that the

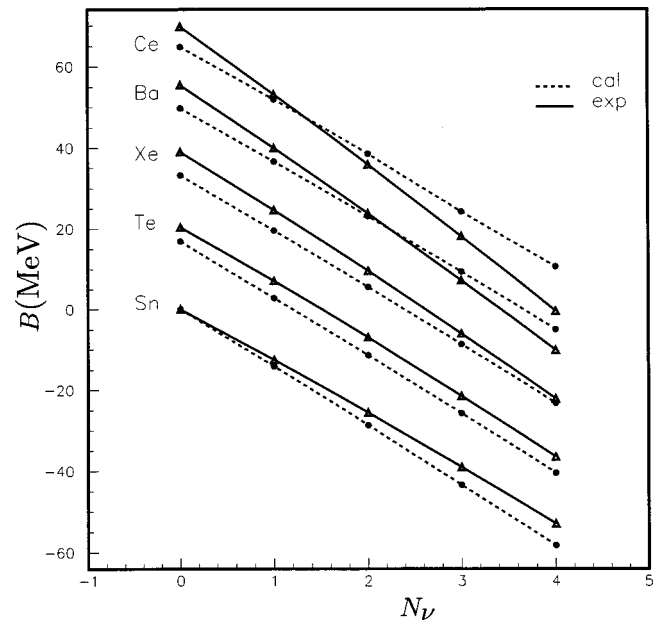


FIG. 3. The relative binding energies B plotted vs the neutron pair number for each isotope. The triangles represent the calculated binding energies in this paper and the dots are experimental data taken from Ref. [25].

single-particle energies, which are very sensitive to the calculated binding energy but determined to be constants using the experimental levels of the nucleus ^{133}Sb (beginning-shell single-particle energies for proton) and those of the nucleus ^{131}Sn (ending-shell single-particle energies for neutron), are not appropriate any more for the nucleus ^{132}Ce where there are eight valence proton particles and eight neutron holes. Anyway, the agreement between the calculated binding energy and the experimental data for the nucleus ^{132}Ce could be improved substantially if one adjusts the monopole pairing strengths and neutron-proton quadrupole-quadrupole interaction strength in a reasonable range.

V. DISCUSSION AND CONCLUSION

In this paper, the excitation energy levels on the ground band and quasibands of doubly even nuclei of around 130 mass region are well described by the simple SD truncation with Hamiltonian (5) by adjusting only two parameters. The relative $E2$ transitions of the nuclei $^{132,134}\text{Ba}$ and ^{130}Xe which were assigned to display the IBM O(6) pattern [23], are reproduced in the calculation. The binding energies are very consistent with the experimental data. The calculated nuclear radii agree well with the results of the RMF calculation. (Note that there are no adjustable parameters in the calculation of nucleus radii.) The strength parameters of the monopole pairing G_σ , quadrupole pairing G_σ^2 , and quadrupole-quadrupole interaction between like nucleons κ_σ , and the neutron-proton quadrupole-quadrupole force κ are comparable with the $P+Q$ parameters [8,21] in this region. It is expected to improve the fitting if we relax the constraints, such as $G_\nu^2 = G_\pi^2$ and $\kappa_\nu = \kappa_\pi$, which are used to reduce the number of free parameters. The nice agreement between the calculated results (energy levels, $E2$ transitions, binding energies, nuclear radii) and the experimental data (or the RMF theory) indicates that the SD nucleon pair approximation is reasonable for most of these nuclei. More data of $E2$ transitions will be helpful to check the validity of the SD approximation of the shell model, and the irregularity of the 6_1^+ states for several nuclei needs further studies.

The consistency of the above calculation encourages us to go further. Since the above SD pair approximation, like the FDSM, carries out all the calculations in fermion space, it is meaningful to compare the results with the FDSM calculation. The advantage of the calculation in this paper is that it has no dynamical symmetry, as a consequence, it can be used to check some assumptions which are made in the FDSM. For example, how the single-particle energy term (splittings) and the abnormal parity contribute to the nuclear collectivity, etc. It has been found [27] that the splittings of single-particle levels would become significant in the low-lying excitations of the nucleus ^{132}Ba if these splittings are artificially enlarged to more than 1.5 times of those observed experimentally, in which case the O(6) behavior of the nucleus would be destroyed. This means that one should be careful in applying the FDSM to realistic nuclei because one cannot be sure in advance that it will produce a correct collective structure. The contribution of the nucleons in the abnormal parity level to nuclear collectivity depends on the

TABLE V. Root of mean-squared radii (ground state). The units are Fermis. The results of the RMF calculation are taken from Table A of Ref. [25].

| Nucl. | ^{132}Te | ^{130}Te | ^{128}Te | ^{126}Te |
|---------------------|-------------------|-------------------|-------------------|-------------------|
| This work (r_p) | 4.705 | 4.693 | 4.681 | 4.662 |
| RMF (r_p) | 4.688 | 4.679 | 4.670 | 4.659 |
| This work (r_n) | 4.988 | 4.960 | 4.931 | 4.864 |
| RMF (r_n) | 4.950 | 4.925 | 4.899 | 4.861 |
| Nucl. | ^{134}Xe | ^{132}Xe | ^{130}Xe | ^{128}Xe |
| This work (r_p) | 4.740 | 4.728 | 4.716 | 4.707 |
| RMF (r_p) | 4.730 | 4.723 | 4.715 | 4.706 |
| This work (r_n) | 5.001 | 4.973 | 4.943 | 4.890 |
| RMF (r_n) | 4.960 | 4.935 | 4.911 | 4.879 |
| Nucl. | ^{136}Ba | ^{134}Ba | ^{132}Ba | ^{130}Ba |
| This work (r_p) | 4.774 | 4.762 | 4.750 | 4.741 |
| RMF (r_p) | 4.770 | 4.763 | 4.754 | 4.745 |
| This work (r_n) | 5.013 | 4.985 | 4.956 | 4.890 |
| RMF (r_n) | 4.976 | 4.944 | 4.915 | 4.887 |
| Nucl. | ^{138}Ce | ^{136}Ce | ^{134}Ce | ^{132}Ce |
| This work (r_p) | 4.806 | 4.793 | 4.792 | 4.788 |
| RMF (r_p) | 4.804 | 4.789 | 4.799 | 4.792 |
| This work (r_n) | 4.997 | 4.976 | 4.934 | 4.917 |
| RMF (r_n) | 4.973 | 4.941 | 4.929 | 4.903 |

structure of the single-particle levels. However, if one uses degenerate single-particle energy levels, the ‘‘loss’’ due to the ignorance of the abnormal parity level can also be restored by parametrizations. Details for these points will be published elsewhere [27].

ACKNOWLEDGMENTS

One of the authors (Y.M.Z.) gratefully acknowledges the Science and Technology Agency of Japan (Contract No. 297040) for supporting this project, and the warm hospitality of the Institute of Modern Physics, Academia Sinica of Lanzhou, and the Institute of Theoretical Physics, Academia Sinica of Beijing. The author would like to thank Professor Nazarewicz and Dr. Meng Jie for discussions, and Dr. G. Maino for communications. Part of the calculations were done on the center machine in RIKEN.

APPENDIX A: SOME TECHNIQUES TO SAVE COMPUTING TIME

The calculation in the SD subspace of the shell model is quite time consuming. The reason is that one cannot use the c.f.p. in the SD pair approximation because the SD pairs are in general not symmetry-dictated nucleon pairs. S_σ , D_σ^\dagger , S_σ^\dagger , D_σ , $\mathcal{P}_\sigma^\dagger$, $\mathcal{P}_\sigma^{(2)}$, and Q_σ do not form a closed algebra. For example, the N -pair overlap $\langle \tau' J_N M_N | \tau J_N M_N \rangle$ can be expressed in terms of many $(N-1)$ -pair overlaps, which

were calculated independently from the beginning using the recursion formulas of Ref. [6], since the subspace is ‘‘open’’ [7,16]. However, in the $(N-1)$ -pair overlaps involved in the N -pair overlap calculation (or the N -pair overlaps involved in the matrix element calculation of Hamiltonian), there is only *one* ‘pair’ [i.e., $A(r'_i)^\dagger \equiv B^{r'_i}$ of Eq. (2.12) in Ref. [6], or $A(r'_i)^\dagger$ of Eqs. (4.6) or (5.3) in the same reference], which can be beyond the original SD subspace. The overlaps of the $(N-1)$ -pair overlaps are closely related to each other. It is unnecessary to calculate *every* $(N-1)$ -pair overlaps from the beginning. This saves the computing time drastically when N becomes large.

For Hamiltonian (5), calculation of V_Q is most time consuming. We notice that the following algorithm to calculate V_Q is much more efficient than Eqs. (5.7) and (5.8) in Ref. [6],

$$\begin{aligned} & \langle \tau' J_N M_N | Q \cdot Q | \tau J_N M_N \rangle \\ &= \sqrt{5} \langle \tau' J_N M_N | [(Q \times Q)^0, A^\dagger(\tau J_N)]_{M_N}^{J_N} | 0 \rangle \\ &= \sqrt{5} \sum_{\tau'' J'_N} \langle \tau' J_N M_N | [Q, A^\dagger(\tau'' J'_N)]_{M_N}^{J'_N} | 0 \rangle, \end{aligned} \quad (\text{A1})$$

where $A^\dagger(\tau'' J'_N) = [Q, A^\dagger(\tau J_N)]_{M_N}^{J'_N}$. The reason why the above formula saves computing time is that the basis $\langle \tau' J_N M_N |$ remains untouched, and only one summation is needed here. In Ref. [6] more summations are needed since both $\langle \tau' J_N M_N |$ and $|\tau' J_N M_N \rangle$ are operated by Q . For example, in the calculation of $\langle DDD, 246 | Q \cdot Q | DDD, 246 \rangle$ [2, 4, and 6 specify J_1 , J_2 , and J_3 , see Eq. (2)], one needs to calculate 4989 nonzero three-pair overlaps using the algorithm of Ref. [6], while only 1717 terms are needed if we use the above equation.

Another improvement to save computing time is to choose the complete basis properly. As was mentioned in Sec. II it is better to choose the possibly *smallest* intermediate angular momenta J_i in the N -pair basis. For the $N=3$ case, it is shown that one can reduce the computing time by about 35% if one chooses the smallest intermediate J_i in the N -pair basis rather than the largest J_i .

APPENDIX B: PARAMETRIZATIONS OF HAMILTONIAN IN THE SD -PAIR APPROXIMATION OF THE SHELL MODEL

In this appendix, we present a collection of parametrizations of Hamiltonians which consists of multipole pairing and quadrupole-quadrupole interactions between like valence nucleons, and quadrupole quadrupole force between valence protons and neutrons.

(1) *Strengths of the multipole pairing interaction.* One must be careful with the definition of the multipole pairing force while talking about pairing strengths. One typical definition is presented in Eqs. (8) and (10). Another frequently used definition of multipole interaction is

$$H_\lambda = -\frac{\pi G_\lambda}{2\lambda+1} \sum_\mu P_{\lambda\mu}^\dagger P_{\lambda\mu}, \quad (\text{B1})$$

where

$$P_{\lambda\mu}^\dagger = \sum_{ab} \langle a || Y^\lambda || b \rangle (C_a^\dagger C_b^\dagger)_M^\lambda. \quad (\text{B2})$$

$\langle a || Y^\lambda || b \rangle$ is the reduced matrix element (Edmond convention) of the spherical harmonics Y_M^λ . The above definition for monopole interaction is the same as Eq. (8). For the quadrupole (or higher-order) pairing interaction, the radial form factor r^λ has been eliminated in the above definition. It was found [21] that the strengths of all the different multipolarities of the pairing residual interaction are approximately the same and equal on average to $G_\lambda \sim 27/A$ MeV ($\lambda=0, 2, 4$, and 6) if one uses the above definition. For realistic cases, guidance values for G_λ for the proton degree of freedom are a bit larger than those for the neutron degree of freedom. For the nuclei calculated in this paper, the $P+Q$ model usually uses $G_0 \sim -0.18$ MeV for the proton, and -0.13 MeV for the neutron.

The definition of quadrupole pairing in Eqs. (11) and (12) has a radial dependence which induces a difference of $\langle nl|r^2|nl' \rangle^2$ in the strength, i.e., $\langle nl|r^2|nl' \rangle^2 G_\sigma^2$ [Eq. (11)] $\sim \pi G_2$ (the above). For nuclei in the $A \sim 130$ region of this paper, $G_\sigma^2 \sim 0.2 G_2$ (MeV/ r_0^4). G_σ^2 in Table II of this paper and Table II of Ref. [14] are close to this value.

(2) *Strengths of the quadrupole-quadrupole force.* Here we make a note on the strengths of κ in Eq. (5) and κ_σ in Eq. (16) for nuclei in this region using the empirical formulas. If one assumes that the deformation is the same for proton and neutron, and that the quadrupole-quadrupole force is a separable force for protons and neutrons, the quadrupole-quadrupole force is

$$H_Q = -\frac{1}{2} \chi (\eta_\pi Q_\pi + \eta_\nu Q_\nu) (\eta_\pi Q_\pi + \eta_\nu Q_\nu), \quad (\text{B3})$$

where $\eta_\sigma = (2Z_\sigma/A)^{2/3}$. For the sake of simplicity, we assume that $\eta_\sigma = 1$. Then the quadrupole-quadrupole force becomes symmetric for the proton and neutron as follows:

$$H_Q = -\frac{1}{2} \chi Q_\pi \cdot Q_\pi - \frac{1}{2} \chi Q_\nu \cdot Q_\nu - \chi Q_\pi Q_\nu. \quad (\text{B4})$$

There are several empirical formulas for the parametrization of χ . Here we list three of them (in units of MeV/ r_0^4) [8]:

$$\begin{aligned} \chi A^{5/3} &= 186, \\ \chi A^{5/3} &= 242 - 10.9 A^{-1/3} (19 - 0.36 Z^2/A), \\ \chi A^{5/3} &= 242 \left[1 + \left(\frac{3}{2} A \right)^{-1/3} \right] - 10.9 A^{-1/3} \\ &\quad \times \left[1 + 2 \left(\frac{3}{2} A \right)^{-1/3} \right] (19 - 0.36 Z^2/A). \end{aligned} \quad (\text{B5})$$

For the nuclei in this paper, $A \sim 132$ and $Z \sim 54$. $\chi \sim 0.054$,

0.064, and $0.073 \text{ MeV}/r_0^4$, respectively, using the above three formulas. The average value can be $\kappa = \chi \sim 2\kappa_\sigma \sim 0.064 \text{ MeV}/r_0^4$. Note that like the multipole pairing interaction, there are also definitions which has no radial form factors in Q . This causes a difference of the strength param-

eter like the multipole pairing interaction. Another minor point is that one should be careful with the definition when $\sqrt{4\pi/(2\lambda+1)}Y_M^\lambda$, when a value other than $Y_{\lambda\mu}$ is in Eq. (13); in this case, there is an additional difference of a constant factor ($4\pi/5$).

-
- [1] A. Arima and F. Iachello, *Ann. Phys. (N.Y.)* **99**, 253 (1976); **111**, 201 (1978); **123**, 468 (1979). For a review, see F. Iachello and A. Arima, *The Interacting Boson Model* (Cambridge University Press, Cambridge, 1987).
- [2] C. L. Wu, D. H. Feng, X. G. Chen, J. Q. Chen, and M. Guidry, *Phys. Rev. C* **36**, 1157 (1987).
- [3] Y. K. Gambir, S. Haq, and J. K. Suri, *Ann. Phys. (N.Y.)* **133**, 154 (1981).
- [4] K. T. Hecht, J. B. McGrory, and J. P. Draayer, *Nucl. Phys.* **A197**, 369 (1972).
- [5] J. Q. Chen, B. Q. Chen, and A. Klein, *Nucl. Phys.* **A554**, 61 (1993); **A562**, 218 (1993).
- [6] J. Q. Chen, *Nucl. Phys.* **A626**, 686 (1997).
- [7] J. Q. Chen and Y. A. Luo, *Nucl. Phys.* **A639**, 615 (1998); J. Q. Chen and X. W. Pan (unpublished).
- [8] M. Baranger and K. Kumar, *Nucl. Phys.* **62**, 113 (1965); *Nucl. Phys.* **A110**, 490 (1968); **A122**, 241 (1968); K. Kumar and M. Baranger, *ibid.* **A110**, 529 (1968); **A122**, 273 (1968). For a review, see, e.g., K. Kumar, *Prog. Part. Nucl. Phys.* **9**, 233 (1983).
- [9] S. Yoshida, *Phys. Rev.* **123**, 2122 (1961).
- [10] B. Q. Chen (unpublished).
- [11] Y. M. Zhao, Ph.D. thesis, Nanjing University, 1995.
- [12] K. Allart, E. Boeker, G. Bonsignori, M. Saroia, and Y. K. Gambhir, *Phys. Rep.* **169**, 209 (1988); I. Talmi, *Nucl. Phys.* **A172**, 1 (1972).
- [13] N. Yoshinaga, T. Mizusaki, A. Arima, and Y. D. Devy, *Prog. Theor. Phys. Suppl.* **125**, 65 (1996).
- [14] T. Mizusaki and T. Otsuka, *Prog. Theor. Phys. Suppl.* **125**, 97 (1996).
- [15] T. Otsuka, A. Arima, and F. Iachello, *Nucl. Phys.* **A309**, 1 (1978).
- [16] Y. M. Zhao and J. Q. Chen, *High Energy Phys. Nucl. Phys.* **21**, 356 (1997); **21**, 438 (1997).
- [17] Y. A. Luo and J. Q. Chen, *Phys. Rev. C* **58**, 589 (1998).
- [18] R. F. Casten and N. V. Zamfir, *J. Phys. G* **22**, 1220 (1996); Y. M. Zhao, *J. Southeast Univ.* **27**, 1 (1997); Y. M. Zhao and Y. Chen, *Phys. Rev. C* **52**, 1453 (1995); Y. Chen, Y. M. Zhao, and J. Q. Chen, *ibid.* **52**, 2520 (1995).
- [19] B. Fogelberg and J. Blomqvist, *Nucl. Phys.* **A429**, 205 (1984).
- [20] W. J. Baldrige, *Phys. Rev. C* **18**, 530 (1978).
- [21] R. A. Broglia, D. R. Bes, and B. S. Nilsson, *Phys. Lett.* **50B**, 213 (1974); H. Sakamoto and T. Kishimoto, *Phys. Lett B* **245**, 321 (1990).
- [22] M. Sakai, *At. Data Nucl. Data Tables* **31**, 399 (1984).
- [23] R. F. Casten and P. Von Brentano, *Phys. Lett.* **152B**, 22 (1985).
- [24] S. Raman, Jr., C. W. Nestor, S. Kahane, and K. H. Bhatt, *At. Data Nucl. Data Tables* **42**, 1 (1989).
- [25] A. H. Wapstra, G. Audi, and R. Hoekstra, *Nucl. Phys.* **A432**, 1 (1985).
- [26] D. Hirata, K. Sumiyoshi, I. Tanihata, Y. Sugahara, and H. Toki (unpublished).
- [27] Y. M. Zhao, N. Yoshinaga, S. Yamaji, and A. Arima, *Phys. Rev. C* **62**, 014316 (2000), following paper.